NASA Technical Memorandum 88949
AIAA-86-0041

Spatially Growing Disturbances in a Two-Stream, Coplanar Jet

Jeffrey H. Miles
Lewis Research Center
Cleveland, Ohio

Prepared for the
24th Aerospace Sciences Meeting
sponsored by the American Institute of Aeronautics and Astronautics
Reno, Nevada, January 6-8, 1986

NASA

SPATIALLY GROWING DISTURBANCES IN A TWO-STREAM, COPLANAR JET

Jeffrey H. Miles

National Aeronautics and Space Administration
Lewis Research Center
Cleveland, Ohio 44135

E-3398

SUMMARY

The influence of the outer stream on the instability of a two-stream, coplanar jet with only the primary (central) stream heated for a nominal outer-to-primary velocity ratio of 0.3 was investigated by means of inviscid linearized stability theory. The instability properties of spatially growing axisymmetric and first order azimuthal disturbances were studied. It was found that the instability characteristics of the two stream jet are very different from those of a single stream jet. The presence of the outer stream enhanced the instability of the jet and increased the unstable frequency range for the first order azimuthal mode.

INTRODUCTION

Improvements in future aircraft operation will be in part due to control and modification of air flow over and about the vehicle. For example, the jet velocity and temperature impinging on the flap surfaces of a short takeoff and landing aircraft employing an under-the-wing blown flap for lift augmentation during takeoff and landing must be controlled in order to maintain flap loads and surface temperatures within acceptable limits for reasons of structural integrity and high-lift performance. Temperature and velocity control is usually achieved through jet mixing with the surrounding medium. Normally mixing is achieved using complex nozzle geometries with consequent weight penalties. Enhanced mixing using acoustic or aero/mechanical excitation devices may reduce this weight penalty. Other situations where acoustic and aero/mechanical excitation may be beneficial are discussed in reference 1.

The effect of excitation on centerline velocity and static temperature decay for a single plume jet is discussed in reference 2. As part of a program to obtain similar information for mixing jets, the unexcited velocity and temperature characteristics of two-stream coplanar jet exhaust plumes was investigated in reference 3. In addition to information on axial velocity and temperature decay, reference 3 also presents typical radial velocity and temperature profiles. In the present paper, these radial and temperature velocity profiles are used as input to a program to analytically determine the phase speed and spatial growth rate of pressure instability waves within the two-stream coplanar jet exhaust plumes.

An excellent review of recent research on the instability of spatially growing disturbances in the free boundary layer of a jet having a single inflection point is presented by Michalke (ref. 4). The two-stream coplanar jet studied herein has two inflection points. As far as the author can determine little work has been done to study free shear layers with two inflection points.

A literature search found only an abstract of a meeting presentation (ref. 5). However, the instability of a circular jet with external flow was analyzed by means of linearized stability theory by Michalke and Herman (ref. 6) and their results show some similarities to the results presented herein.

For the Mach number range of the present study (around M = 0.9), the flow is compressible. The instability of spatially growing disturbances propagating insentropically in a circular jet for flow in this Mach number range was studied by Michalke (ref. 7) and Morris (ref. 8).

In this study, viscous effects and effects due to the slowly diverging jet flow (refs. 9 to 11) are neglected. Furthermore, the analysis follows that of Michalke (ref. 7) where it was assumed that disturbances propagate isentropically.

Measurements of modal structure show that the large scale structure of turbulence in a circular jet where the velocity profile has only a single inflection point is dominated by the axisymmetric and first order azimuthal components (ref. 12). Consequently, at a minimum the axisymmetric and first order azimuthal components of the disturbance in circular jets are studied in all theoretical investigations. Although in this study the jet velocity profile has two inflection points, the stability calculations are still restricted to these two components.

NOMENCLATURE

a	speed of sound, m/s
B	see eq. (1)
C_e	amplitude coefficient, see eq. (15)
c	wave velocity, β/α, m/s
c_{ph}	phase velocity, β/α_r, m/s
f	eigenfunction
$F(r,B,\delta)$	radial profile term
$G(r)$	velocity profile shape
$H(\alpha\theta)$	eigenvalue equation
i	$\sqrt{-1}$
m	azimuthal wavenumber
p	pressure
r	radial position
R	radius
T	static temperature

t	time, sec
U	mean nozzle exit centerline velocity
U_{clx}	mean velocity on centerline at a given x/D_p
u,v,w	velocity components
x	axial position
α	complex eigenvalue wavenumber
β	radian frequency
Δu	velocity difference, $U_{clx} - U_\infty$
δ	see eq. (1)
θ	shear layer momentum thickness
λ	see eq. (9)
ρ	density
φ	cylindrical angular coordinate

Subscripts

c	compressible
clx	center line at a given x/D position
e	exterior solution
h	meeting point
i	imaginary
P	primary jet
r	real
s	secondary or outer stream
T	temperature related
0	interior solution
∞	ambient

Superscript

(~) scaled quantity

( )' small disturbance

THEORY

Jet Velocity and Temperature Characteristics

In order to determine the stability of the disturbances, the radial distribution of mean velocity and temperature in the two-stream axisymmetric jet must be specified. The condition selected for study is one of the cases presented in reference 3. For this case, the nominal primary jet Mach number is 0.9, the nominal outer-to-primary velocity ratio is 0.3, and only the primary stream is heated. The nozzle used for this case had a secondary to primary flow area ratio of 1.9 since the primary nozzle diameter is 10 cm, the secondary nozzle diameter is 17.6 cm, and the primary nozzle thickness is 0.46 cm. The nozzle dimensions, jet velocities, and temperatures are shown in table I.

Mathematical expressions for the velocity and temperature profiles were constructed using a basic profile function. The basic function used is

$$F(r,B,\delta) = \frac{1}{2}\left\{1 + \tanh\left[B\left(1 - \frac{r}{\delta R}\right)\right]\right\} \tag{1}$$

where the constants B and δ are determined from experimental data.

Since the flow configuration studied consist of two flow streams, it is not surprising that a reasonable curve fit to the experimental velocity profile could be achieved by adding together two separate functions specified by equation (1) with appropriate constants and appropriate weighting coefficients. The resulting equation for the curve fit to the velocity profile is

$$G_U(r) = \left(1 - \frac{U_s}{U_p}\right) F\left(r,B_{U_p},\delta_{U_p}\right) + \frac{U_s}{U_p} F\left(r,B_{U_s},\delta_{U_s}\right) \tag{2}$$

The velocity profile for the primary and secondary jets have a "top hat profile" near the nozzle. Consequently, near the nozzle the values of B are large ($B_{U_p} = 10$ and $B_{U_s} = 10$) and on the centerline $G_U(0)$ is unity. However, at large x/D_p the profiles are broad and the values of B are nearer unity. When the values of B are near unity, then the value of $G(0)$ is not unity. Since the experimental data of reference 3 was normalized by the jet centerline velocity, on the jet centerline the velocity profile calculated using the curve fit equation (eq. (2)) must also have a value of unity. Consequently, the basic shape is normalized by dividing by $G_U(0)$. Thus the actual velocity profile used is

$$\frac{U(r)}{U_{clx}} = \frac{G_U(r)}{G_U(0)} \tag{3}$$

where U_{clx} is the mean velocity on the centerline at a given x/D_p position. The constants used were determined by curve fitting data given in reference 3 and they are shown in table I. The resulting curve fits to the velocity data are compared with the actual data in figure 1.

The equation used to curve fit the experimental temperature profile for the case with a cold secondary is

$$G_T(r) = F\left(r, B_{T_p}, \delta_{T_p}\right) \tag{4}$$

Note, the temperature profile has only a single inflection point since the outer stream temperature is near the temperature of the surrounding air. Again, the temperature profiles are normalized by the centerline temperature. Consequently, the temperature profile used for this case is normalized by $G_T(0)$

$$\frac{T(r) - T_\infty}{T_{clx} - T_\infty} = \frac{G_T(r)}{G_T(0)} \tag{5}$$

The constants used were determined by curve fitting data given in reference 3 and they are shown in table I. The resulting curve fits to the temperature data are compared with the measured data in figure 2.

The shear layer momentum thickness, θ_c, is used as the characteristic of the free jet shear layer. For compressible flow, it is defined as follows:

$$\theta_c = \int_0^\infty \frac{P(r)}{P_{clx}} \frac{U(r)}{U_{clx}} \left(1 - \frac{U(r)}{U_{clx}}\right) dr \tag{6}$$

Note, however, that the incompressible shear layer momentum thickness defined as

$$r = \int_0^\infty \frac{U(r)}{U_{clx}} \left(1 - \frac{U(r)}{U_{clx}}\right) dr \tag{7}$$

is more frequently used to characterize the thickness of the velocity shear layer for jet shear layer instability studies even for compressible flow (ref. 4). Consequently, it is used again in this paper. For each axial position both shear layer momentum thickness characterizations are shown in table I.

LINEARIZED DISTURBANCE EQUATIONS

The disturbance equations are derived by introducing small disturbances u', v', w', p', and ρ' into the equations of momentum and mass conservation and keeping only the linear terms. The equations are linearized about the basic jet flow which is assumed to be locally parallel with $U(r)$ being the axial mean velocity component of the undisturbed flow. The Reynolds number of the flow is assumed to be large so that the unsteady flow is inviscid. The flow is also assumed to be isentropic.

The disturbance is assumed to be a spatially growing wave of the type

$$[u',v',w',p',\rho'] = [u(r),v(r),w(r),p(r),\rho(r)]\,x[\exp i(\alpha x - m\varphi - \beta t)] \tag{8}$$

where the radian frequency, β, and the integer azimuthal wave number, m, are real, while the eigenvalue wavenumber, α, is complex. The real value of α, α_r, is the axial wave number. The imaginary value of α determines the spatial growth rate, $-\alpha_i$. If $-\alpha_i$ is greater than zero, the wave defined by equation (8) grows as it propagates. The propagation phase velocity, c_{ph}, is given by β/α_r.

Using equation (8), the disturbance equations can be reduced to a single differential equation for the radial pressure perturbation function, p(r):

$$\frac{d^2P}{dr^2} + \left\{ \frac{1}{r} - \frac{2}{\left[U(r) - \frac{\beta}{\alpha}\right]} \frac{dU(r)}{dr} \right\} \frac{dp}{dr} - \left[\alpha^2\lambda^2(r) + \frac{m^2}{r^2}\right] P = 0 \tag{9}$$

where

$$\lambda^2(r) = 1 - \left[\frac{U(r) - \frac{\beta}{\alpha}}{a}\right]^2$$

and a is the acoustic speed of sound. Equations of this form for the fluctuating pressure are well known and given in references 7 and 8.

Near the jet axis ($r \to 0$) and also in the ambient fluid far from the jet ($r \to \infty$) the velocity profile, U(r), is flat and dU(r)/dr is zero. In these regions, equation (9) reduces to a form of the Bessel equation. Consequently, the asymptotic solutions to equation 9 are given by the modified Bessel functions I_m and K_m of order m. The boundary conditions for the pressure require that p(0) has to be bounded and $p(\infty)$ has to be zero. Hence, near the jet axis ($r \to 0$)

$$p(r) \cong I_m\,[\alpha\lambda(r)r] \tag{10}$$

and in the ambient fluid ($r \to \infty$)

$$p(r) \cong K_m\,[\alpha\lambda(r)r] \tag{11}$$

The numerical procedure used to solve the eigenvalue problem is a shooting method similar to that described in referece 7. Equation (9) is scaled using the incompressible momentum boundary layer thickness, θ, and the velocity difference, ΔU, between the jet centerline velocity, $U_{c_{1x}}$, at a particular x/D, and the ambient jet velocity, U_∞. For the case studied, ΔU is identical with the jet centerline velocity, $U_{c_{1x}}$ since the ambientvelocity is zero. The resulting differential equation is

$$\frac{d^2P}{d\tilde{r}^2} + \left[\frac{1}{\tilde{r}} - \frac{2}{\left[\tilde{U} - \left(\frac{\beta\theta}{\Delta U}\right)\left(\frac{1}{\alpha\theta}\right)\right]} \frac{d\tilde{U}}{d\tilde{r}}\right] \frac{dp}{d\tilde{r}} - \left[(\alpha\theta)^2\lambda^2 + \frac{m^2}{\tilde{r}^2}\right] P = 0 \tag{12}$$

where

$$\lambda^2 = 1 - \left[\frac{\tilde{U} - \left(\frac{\beta\theta}{\Delta U}\right)\left(\frac{1}{\alpha\theta}\right)}{\frac{a}{\Delta U}}\right]^2$$

and the dimensionless radial length, $\tilde{r}$, and dimensionless velocity, $\tilde{U}$, are

$$\tilde{r} = \frac{r}{\theta}$$

and

$$\tilde{U} = \frac{U}{\Delta U} = \frac{U}{U_{c1x}}$$

This equation depends on two normalized parameters, the dimensionless wave number $\alpha\theta$ and the dimensionless frequency or Strouhal number, $\beta\theta/\Delta U$.

The complex differential equation written as a first order vector system is integrated numerically by a Runge-Kutta procedure. The infinite integration region is divided into two finite regions, an inner region $\tilde{r}_0 < \tilde{r} < \tilde{r}_h$ and an outer region $\tilde{r}_h < \tilde{r} < \tilde{r}_\infty$. The values of $\tilde{r}_0$ and $\tilde{r}_\infty$ are chosen to insure that $d\tilde{U}/d\tilde{r}$ is small and the integration of equation (12) can be started at these points.

In the inner region

$$P_0(\tilde{r}) = f_0(\tilde{r}) \tag{13}$$

where $f_0(\tilde{r})$ represents the numerical Runge-Kutta solution in the inner region. Considering equation (10), the proper initial condition for Runge-Kutta integration starting near the origin is

$$P_0(\tilde{r}_0) = \left[\alpha\theta\lambda(\tilde{r}_0)\tilde{r}_0\right] \tag{14}$$

In the outer region, the numerical Runge-Kutta solution is given by

$$P_e(\tilde{r}) = C_e f_e(\tilde{r}) \tag{15}$$

In contrast to the inner region, the Runge-Kutta solution is obtained by integrating from $\tilde{r}_\infty$ toward the origin. Far from the jet, from equation (11), the proper initial condition for the Runge-Kutta integration from $\tilde{r}_\infty$ to $\tilde{r}_h$ is

$$P_e\left(\tilde{r}_\infty\right) = C_e K_m \left[\alpha\theta\lambda(\tilde{r}_\infty)\tilde{r}_\infty\right] \tag{16}$$

The eigenvalue is determined by an iterative procedure. The eigenvalue is the value of α which makes p and $dp/d\tilde{r}$ continuous at $\tilde{r} = \tilde{r}_h$. Hence, the eigenvalue equation for $\alpha\theta$ is

$$H(\alpha\theta) = f_0(\tilde{r}_h) \frac{df_e(\tilde{r}_h)}{d\tilde{r}} - f_e(\tilde{r}_h) \frac{df_0(\tilde{r}_h)}{d\tilde{r}} = 0 \qquad (17)$$

where f_0 and $C_e f_e$ are the solutions in the inner and outer regions. The constant C_e is determined by the condition that at $\tilde{r}_h$ the inner and outer pressure eigenfunction solutions have the same value.

The eigenvalue is determined in a two step procedure. The first step uses a technique employed in reference 13. The technique is based on a theorem in complex variable theory which states that the number of zeros within a closed contour equals the net multiples of 2π by which the phase angle of $H(\alpha\theta)$ changes around the contour (ref. 14). Initially a rectangular contour was used. This procedure found regions where there were no eigenvalues or regions which contained eigenvalues. In addition, an examination of the variation of the value of the magnitude of $H(\alpha\theta)$ determined as one followed a closed contour produced useful information on the location of possible eignevalues even if none were located inside the closed contour. The method produces a good initial guess which is then used by a least squares function minimization iterative procedure that finds the eigenvalue by minimizing $H(\alpha\theta)$. Using a circular contour centered near a suspected eigenvalue and incrementally reducing the radius of the contour, provides a means of insuring a true eigenvalue is found rather than a local minimum of $H(\alpha\theta)$.

RESULTS

Using the curve fit velocity functions, $\tilde{U} = U/U_{c1x}$, the eigenvalues, growth rates, and phase velocities were calculated for the axisymmetric mode at $x/D_p = 1$, 4, and 8 and for the first order azimuthal mode at $x/D_p = 1$, 4, 8, and 12.75. These results are presented in table II. The spatial growth and phase velocities are shown in figures 3 to 6.

Figure 3 shows the dimensionless spatial growth rate, $-a_i\theta$, as a function of the Strouhal number, $\beta\theta/\Delta U$, at $x/D_p = 1$, 2, and 4 for the axisymmetric ($m = 0$) disturbance and at $x/D_p = 1$, 2, 4, 8, and 12.75 for the first azimuthal ($m = 1$) disturbances. At all frequencies and for $x/D_p = 1$, 2, and 4, the first azimuthal disturbances have a greater growth rate than that of the axisymmetric mode. The range of unstable frequencies for the first azimuthal disturbance is also greater than the range of unstable frequencies for the axisymmetric jet.

In figure 4, the relative axial phase velocity, $c_{ph}/\Delta U$ is plotted as a function of the Strouhal number for $m = 0$ at $x/D_p = 1$, 2, and 4, and for $m = 1$ at $x/D_p = 1$, 2, 4, 8, and 12.75. For the two-stream axisymmetric jet, the phase velocity of the axisymmetric disturbance ($m = 0$) always decreases with increasing frequency from the jet velocity U_{c1x} at a frequency of zero. Also, the phase velocity of the first azimuthal disturbance ($m = 1$) is always less than the phase velocity of the axisymmetric disturbance ($m = 0$).

Thus the frequency dependence of the phase velocities of the axisymmetric and first azimuthal disturbances are similar to those shown for a single jet in reference 6.

The results shown in figure 3 are replotted in figure 5 to show the spatial growth rates at various x/D_p values for $m = 0$ and $m = 1$. Clearly, the use of velocity profiles that depend on five parameters yields sets of growth rate curves with complicated behavior. These results are a function of the curve fit and the measured velocity and temperature data. An improved curve fit, a curve fit based on different functional form, or a curve fit based on more extensive data will give different results. A sensitivity analysis was not performed.

Figure 5(a) shows that for the axisymmetric mode ($m = 0$) the growth rate at Strouhal numbers less than 0.05 is largest at $x/D_p = 1$, while for Strouhal numbers from 0.05 to 0.175 the growth rate is largest at $x/D_p = 2$, and for frequencies greater than 0.715 the growth rate is largest at $x/D_p = 4$. However, the magnitude of the growth rate is larger at $x/D_p = 2$ than at $x/D_p = 1$ or $x/D_p = 4$.

Figure 5(b) shows that for the first azimuthal mode ($m = 1$) the growth rate is largest at $x/D_p = 1$. For each axial position except $x/D_p = 8$ the Strouhal number at which the growth rate curve peaks decreases as x/D_p increases. The growth rate at $x/D_p = 8$ is greater than the growth rate at $x/D_p = 4$.

The relative phase velocity at various x/D_p values for $m = 0$ and $m = 1$ are 6ompared in figure 6. The complicated velocity profiles that depend on five parameters also yield sets of phase velocity curves with complicated behavior. Figure 6(a) shows that for the axisymmetric mode ($m = 0$) the relative phase velocity decreases from 1 to about 0.7 for $x/D_p = 1$, 2, and 4. However, the rate of change is very large at $x/D_p = 1$ and more gradual at $x/D_p = 2$ and 4.

Figure 6(b) shows that for the first azimuthal mode ($m = 1$) the relative phase velocity at low Strouhal numbers is largest for $x/D_p = 1$ and becomes progressively smaller as x/D_p increases. However, at higher Strouhal numbers the phase velocity at $x/D_p = 12.75$ is greater than the phase velocity at $x/D_p = 8$ and the phase velocity at $x/D_p = 2$ is greater than the phase velocity at $x/D_p = 1$.

DISCUSSION

These results indicate aero/mechanical excitation of a two-stream coplanar jet operating at a secondary to primary velocity ratio of 0.3 using devices that perturb only the axisymmetric mode would not be as effective as using devices that perturb the first order azimuthal mode. Furthermore, these calculations are indicative of those that may be necessary in order to properly prepare an experimental test program to develop aero/mechanical excitation devices.

In addition, the two-stream, coplanar jet results differ in many respects from those presented by Michalke and Herman (ref. 6). In that study of the influence of external flow velocity on jet stability of a single jet, the following velocity profile was used

$$U(r) = U_\infty + \frac{1}{2}\Delta U\left\{1 - \tanh\left[\frac{R}{4\theta}\left(\frac{r}{R} - \frac{R}{r}\right)\right]\right\} \qquad (18)$$

where U_∞ is an external flow velocity, and $\Delta U = U_{c1x} - U_\infty$.

The most striking difference observed in comparing the two-stream, coplanar jet results with those obtained for the static case of reference 6 ($U_\infty = 0$) is that for the coplanar jet the first azimuthal mode is more unstable than the axisymmetric mode at all x/D. In addition, for the first azimuthal disturbance the neutral stability point is at a much higher frequency and the magnitude of the growth rate is greater for the coplanar jet.

In order to determine the affects of the secondary flow for the first azimuthal mode (m = 1) case, a test calculation was made using the velocity profile of the primary jet without any secondary flow. These results are given in table III and are shown in figures 7 and 8. Figure 7 compares the spatial growth rate of the primary jet with the spatial growth rate of the two-stream jet. Note the magnitude of the growth rate is unchanged while the calculations made using the secondary jet peaks at a higher frequency and has a much higher neutral stability frequency. This increased region of unstable frequencies and the shift of the peak of the spatial growth rate to higher frequencies is similar to that observed in reference 6 for those cases where the external flow velocity was not zero. Figure 8 compares the phase velocities for the same cases.

CONCLUDING REMARKS

It has been shown that the instability characteristics of the two-stream axisymmetric jet are considerably different from those of a single stream jet. The presence of the secondary stream enhanced the instability of the first order azimuthal mode and extended the frequency range at which it occurred. For a two-stream, coplanar jet operating at a secondary to primary velocity ratio of 0.30 aero/mechanical excitation should be designed to excite the first order azimuthal mode and not just the axisymmetric mode to increase mixing.

REFERENCES

1. Stone, J.R. and McKinzie, D.J., Jr. "Acoustic Excitation--A Promising New Means of Controlling Shear Layers," NASA-TM 83772, 1984.

2. von Glahn, U.H., "On Some Flow Characteristics of Conventional and Excited Jets," AIAA Paper 84-0532, Jan. 1984.

3. von Glahn, U., Goodykoontz, J., and Wasserbauer, C., "Velocity and Temperature Characteristics of Two-Stream, Coplanar Jet Exhaust Plumes," AIAA Paper 84-2205, Aug. 1984.

4. Michalke, A., "Survey on Jet Instability Theory," Progress in Aerospace Sciences, Vol. 21, No. 3, 1984, pp.159-199.

5. Crighton, D. G., "Instability and Acoustic Properties of Coaxial Jets," Bulletin of the American Physical Society, Vol. 29, No. 4, 1984, AE1.

6. Michalke, A. and Hermann, G., "On the Inviscid Instability of a Circular Jet with External Flow," Journal of Fluid Mechanics, Vol. 114, Jan. 1982, pp. 343-359.

7. Michalke, A., "Instibilitat eines kompressiblen runden Frestrahls unter Berucksichtigung des Einflusses der Strahlgrenzschichtdicke," Zeitschrift fur Flugwissenchaften, Vol. 19, No. 8/9, Aug./Sept. 1971, pp. 319-328.

8. Morris, P.J., "Flow Characteristics of the Large Scale Wave-Like Structure of a Supersonic Round Jet," Journal of Sound and Vibration, Vol. 53, No. 2, July 22, 1977 pp. 223-244.

9. Morris, P.J., "The Spatial Instability of Axisymmetric Jets," Journal of Fluid Mechanics, Vol. 77, Part 3, Oct. 8, 1976, pp. 511-529.

10. Crighton, D.G. and Gaster, M., "Stability of Slowly Diverging Jet Flow.," Journal of Fluid Mechanics, Vol. 77, Part 2, Sept. 24, 1976, pp. 397-413.

11. Plaschko, P., "Helical Instabilities of Slowly Diverging Jets," Journal of Fluid Mechanics, Vol. 92, Part 2, May 28, 1979, pp. 209-215.

12. Stromberg, J.L., McLaughlin, D.K., and Troutt, T.R. "Flow Field and Acoustic Properties of a Mach Number 0.9 Jet at Low Reynolds Number," Journal of Sound and Vibration, Vol. 72, No. 2. Sept. 22, 1980, pp. 159-176.

13. Lessen, M., Sadler, S.G., and Liu, T.-Y., "Stability of Pipe Poiseuille Flow," Physics of Fluids, Vol. 11, No. 7, July 1968, pp 1404-1409.

14. Kaplan, W., "Operational Methods for Linear Systems," Addison-Wesley, Reading, MA, 1962, pp. 157-158.

TABLE I. - JET TEST CONDITIONS AND PROFILE PARAMETERS

Exit Mach number	0.94
Primary jet nozzle diameter, cm	10
Secondary or outer jet nozzle diameter, cm	17.6
Primary jet nozzle wall thickness, cm	.46
Secondary to primary nozzle area ratio	1.9
Primary jet exit velocity, m/s	598
Secondary jet exit velocity, m/s	174
Primary jet exit temperature, K	984
Secondary jet exit temperature, K	285

$\frac{x}{D_p}$	$\frac{R_p}{\theta}$	θ, cm	θ_c, cm	U_{clx}, m/s	T_{clx}, K	B_{U_p}	δ_{U_p}	B_{U_s}	δ_{U_s}	B_T	δ_{T_p}
1	11	0.899	3.17	598	984	10	1.1	10	1.8	10	0.9
2	8	1.22	3.55	598	984	6.3	1.1	6.3	2.	6	1.1
4	7	1.46	4.05	546	984	3.6	1.1	3.6	2.	3	1
8	4	2.51	5.38	537	856	1.5	.9	1.5	2.2	1	.9
12.75	3	3.23	5.24	366	639	1.2	1.2	1.2	2.5	.8	1.3

TABLE II. - TWO-STREAM, COPLANAR JET EIGENVALUES, GROWTH RATES, AND PHASE VELOCITIES

(a) $x/D_p = 1$, Axisymmetric mode (m = 0)

	$\frac{\alpha\theta}{\Delta U}$	$\frac{c_r}{\Delta U}$	$\frac{c_i}{\Delta U}$	$\alpha_r\theta$	$\alpha_i\theta$	$\frac{c_{ph}}{\Delta U}$
1	0.010	0.9824	1.1145E-01	0.0100	-1.1401E-03	0.9950
2	.020	.8273	2.3523E-01	.0224	-6.3600E-03	.8942
3	.030	.7442	1.5855E-01	.0386	-8.2157E-03	.7780
4	.040	.7275	1.2193E-01	.0535	-8.9641E-03	.7479
5	.050	.7219	1.0104E-01	.0679	-9.5083E-03	.7360
6	.060	.7203	8.6026E-02	.0821	-9.8079E-03	.7306
7	.070	.7190	7.4581E-02	.0963	-9.9914E-03	.7267
8	.080	.7197	6.1686E-02	.1103	-9.4581E-03	.7250
9	.090	.7199	4.4335E-02	.1245	-7.6697E-03	.7226
10	.100	.7206	1.9589E-02	.1387	-3.7692E-03	.7212

TABLE II. - Continued.

(b) x/D_p = 1, First azimuthal mode (m = 1)

	$\frac{\alpha\theta}{\Delta U}$	$\frac{c_r}{\Delta U}$	$\frac{c_i}{\Delta U}$	$\alpha_r\theta$	$\alpha_i\theta$	$\frac{c_{ph}}{\Delta U}$
1	0.010	0.5681	3.2871E-01	0.0132	-7.6301E-03	0.7583
2	.020	.5640	3.1912E-01	.0269	-1.5198E-02	.7446
3	.030	.5606	3.0264E-01	.0414	-2.2370E-02	.7240
4	.040	.5619	2.8175E-01	.0569	-2.8520E-02	.7032
5	.050	.5687	2.6118E-01	.0726	-3.3340E-02	.6887
6	.060	.5787	2.4360E-01	.0881	-3.7073E-02	.6813
7	.070	.5897	2.2921E-01	.1031	-4.0078E-02	.6788
8	.080	.6008	2.1746E-01	.1177	-4.2612E-02	.6795
9	.090	.6115	2.0785E-01	.1319	-4.4842E-02	.6822
10	.100	.6218	2.0003E-01	.1457	-4.6887E-02	.6861
11	.110	.6316	1.9388E-01	.1592	-4.8858E-02	.6911
12	.120	.6410	1.8949E-01	.1722	-5.0898E-02	.6970
13	.130	.6497	1.8714E-01	.1848	-5.3225E-02	.7036
14	.140	.6569	1.8711E-01	.1971	-5.6154E-02	.7102
15	.150	.6613	1.8883E-01	.2097	-5.9890E-02	.7152
16	.160	.6623	1.9038E-01	.2231	-6.4139E-02	.7171
17	.170	.6613	1.9027E-01	.2374	-6.8315E-02	.7160
18	.180	.6595	1.8841E-01	.2523	-7.2080E-02	.7134
19	.190	.6579	1.8534E-01	.2676	-7.5370E-02	.7101
20	.200	.6567	1.8159E-01	.2829	-7.8236E-02	.7069
21	.210	.6558	1.7752E-01	.2984	-8.0757E-02	.7039
22	.220	.6553	1.7334E-01	.3138	-8.3004E-02	.7011
23	.230	.6550	1.6920E-01	.3292	-8.5034E-02	.6987
24	.240	.6549	1.6515E-01	.3446	-8.6895E-02	.6965
25	.250	.6549	1.6124E-01	.3599	-8.8619E-02	.6946
26	.260	.6550	1.5748E-01	.3753	-9.0233E-02	.6928
27	.270	.6550	1.5386E-01	.3906	-9.1753E-02	.6912
28	.280	.6551	1.5037E-01	.4060	-9.3190E-02	.6897
29	.290	.6552	1.4701E-01	.4214	-9.4548E-02	.6882
30	.300	.6552	1.4375E-01	.4368	-9.5833E-02	.6868
31	.310	.6565	1.4071E-01	.4514	-9.6755E-02	.6867
32	.320	.6552	1.3750E-01	.4678	-9.8174E-02	.6840
33	.330	.6551	1.3447E-01	.4834	-9.9221E-02	.6827
34	.340	.6549	1.3148E-01	.4990	-1.0018E-01	.6813
35	.350	.6548	1.2853E-01	.5147	-1.0104E-01	.6800
36	.360	.6546	1.2561E-01	.5305	-1.0180E-01	.6787
37	.370	.6543	1.2270E-01	.5463	-1.0244E-01	.6773
38	.380	.6540	1.1981E-01	.5621	-1.0297E-01	.6760
39	.390	.6538	1.1692E-01	.5781	-1.0338E-01	.6747
40	.400	.6535	1.1403E-01	.5940	-1.0366E-01	.6734
41	.410	.6532	1.1115E-01	.6100	-1.0380E-01	.6721
42	.420	.6529	1.0827E-01	.6260	-1.0381E-01	.6709
43	.430	.6540	1.0561E-01	.6408	-1.0349E-01	.6710
44	.440	.6524	1.0251E-01	.6582	-1.0341E-01	.6685
45	.450	.6522	9.9635E-02	.6743	-1.0301E-01	.6674
46	.460	.6520	9.6767E-02	.6903	-1.0246E-01	.6663
47	.470	.6518	9.3905E-02	.7064	-1.0178E-01	.6653

Table II. - Continued.

(b) Concluded

	$\frac{\alpha\theta}{\Delta U}$	$\frac{c_r}{\Delta U}$	$\frac{c_i}{\Delta U}$	$\alpha_r\theta$	$\alpha_i\theta$	$\frac{c_{ph}}{\Delta U}$
48	0.480	0.6516	9.1054E-02	0.7225	-1.0096E-01	0.6644
49	.490	.6515	8.8213E-02	.7386	-1.0000E-01	.6634
50	.500	.6514	8.5385E-02	.7546	-9.8916E-02	.6626
51	.550	.6513	7.1485E-02	.8345	-9.1593E-02	.6591
52	.560	.6513	6.8760E-02	.8503	-8.9770E-02	.6586
53	.570	.6526	6.6373E-02	.8645	-8.7930E-02	.6593
54	.580	.6515	6.3370E-02	.8819	-8.5785E-02	.6577
55	.590	.6516	6.0706E-02	.8977	-8.3629E-02	.6573
56	.600	.6517	5.8064E-02	.9134	-8.1370E-02	.6569
57	.610	.6531	5.5769E-02	.9273	-7.9185E-02	.6578
58	.620	.6521	5.2843E-02	.9446	-7.6545E-02	.6564
59	.630	.6523	5.0263E-02	.9601	-7.3983E-02	.6562
60	.640	.6525	4.7707E-02	.9756	-7.1330E-02	.6560
61	.650	.6527	4.5169E-02	.9911	-6.8580E-02	.6559
62	.660	.6530	4.2655E-02	1.0064	-6.5743E-02	.6558
63	.670	.6533	4.0160E-02	1.0218	-6.2816E-02	.6557
64	.680	.6535	3.7690E-02	1.0371	-5.9810E-02	.6557

Table II. - Continued.

(c) $x/D_p = 1$, Axisymmetric mode ($m = 0$)

	$\frac{\alpha\theta}{\Delta U}$	$\frac{c_r}{\Delta U}$	$\frac{c_i}{\Delta U}$	$\alpha_r\theta$	$\alpha_i\theta$	$\frac{c_{ph}}{\Delta U}$
1	0.010	0.9969	2.6240E-02	0.0100	-2.6384E-04	0.9976
2	.020	.9935	5.3769E-02	.0201	-1.0862E-03	.9964
3	.030	.9888	-8.4064E-02	.0301	2.5611E-03	.9959
4	.040	.9809	1.1962E-01	.0402	-4.9004E-03	.9955
5	.050	.9636	1.6341E-01	.0504	-8.5536E-03	.9913
6	.060	.9196	2.1091E-01	.0620	-1.4217E-02	.9679
7	.070	.8479	2.2116E-01	.0773	-2.0164E-02	.9055
8	.080	.8010	1.9918E-01	.0941	-2.3392E-02	.8505
9	.090	.7755	1.7576E-01	.1104	-2.5017E-02	.8154
10	.100	.7604	1.5634E-01	.1262	-2.5940E-02	.7926
11	.110	.7507	1.4051E-01	.1416	-2.6501E-02	.7770
12	.120	.7439	1.2740E-01	.1567	-2.6836E-02	.7658
13	.130	.7391	1.1627E-01	.1716	-2.6999E-02	.7574
14	.140	.7366	1.0607E-01	.1862	-2.6810E-02	.7519
15	.140	.7366	1.0607E-01	.1862	-2.6809E-02	.7519
16	.150	.7329	9.7991E-02	.2011	-2.6881E-02	.7460
17	.160	.7309	9.0134E-02	.2156	-2.6590E-02	.7420
18	.170	.7294	8.2791E-02	.2301	-2.6121E-02	.7388
19	.180	.7281	7.5759E-02	.2446	-2.5447E-02	.7360
20	.190	.7271	6.8862E-02	.2590	-2.4530E-02	.7336
21	.200	.7261	6.1936E-02	.2735	-2.3326E-02	.7314
22	.210	.7250	5.4835E-02	.2880	-2.1783E-02	.7292
23	.220	.7236	4.7451E-02	.3027	-1.9853E-02	.7267
24	.230	.7215	3.9775E-02	.3178	-1.7522E-02	.7237
25	.240	.7183	3.2022E-02	.3335	-1.4865E-02	.7197
26	.250	.7133	2.1040E-02	.3502	-1.0329E-02	.7139
27	.260	.7072	1.5199E-02	.3675	-7.8980E-03	.7075
28	.270	.7009	1.0784E-02	.3851	-5.9254E-03	.7011
29	.280	.6948	7.5130E-03	.4029	-4.3569E-03	.6949
30	.290	.6894	4.8693E-03	.4206	-2.9708E-03	.6895
31	.300	.6871	3.8678E-03	.4366	-2.4578E-03	.6871
32	.310	.6871	3.4261E-03	.4512	-2.2496E-03	.6871
33	.320	.6871	3.1899E-03	.4657	-2.1620E-03	.6871

Table II. - Continued.

(d) $x/D_p = 1$, First azimuthal mode ($m = 1$)

	$\frac{\alpha\theta}{\Delta U}$	$\frac{c_r}{\Delta U}$	$\frac{c_i}{\Delta U}$	$\alpha_r\theta$	$\alpha_i\theta$	$\frac{c_{ph}}{\Delta U}$
1	0.010	0.5720	2.8965E-01	0.0139	-7.0456E-03	0.7187
2	.020	.5707	2.8447E-01	.0281	-1.3993E-02	.7125
3	.030	.5694	2.7586E-01	.0427	-2.0673E-02	.7030
4	.040	.5695	2.6439E-01	.0578	-2.6829E-02	.6922
5	.050	.5718	2.5139E-01	.0733	-3.2218E-02	.6823
6	.060	.5764	2.3836E-01	.0889	-3.6760E-02	.6750
7	.070	.5826	2.2631E-01	.1044	-4.0549E-02	.6705
8	.080	.5897	2.1558E-01	.1197	-4.3746E-02	.6685
9	.090	.5971	2.0617E-01	.1347	-4.6498E-02	.6683
10	.100	.6045	1.9791E-01	.1494	-4.8918E-02	.6693
11	.110	.6117	1.9063E-01	.1639	-5.1088E-02	.6711
12	.120	.6185	1.8420E-01	.1782	-5.3069E-02	.6734
13	.130	.6251	1.7850E-01	.1923	-5.4908E-02	.6761
14	.140	.6314	1.7345E-01	.2062	-5.6645E-02	.6790
15	.150	.6373	1.6902E-01	.2199	-5.8319E-02	.6821
16	.160	.6430	1.6519E-01	.2334	-5.9974E-02	.6854
17	.170	.6483	1.6198E-01	.2468	-6.1664E-02	.6888
18	.180	.6533	1.5943E-01	.2600	-6.3455E-02	.6922
19	.190	.6579	1.5760E-01	.2731	-6.5432E-02	.6956
20	.200	.6618	1.5651E-01	.2862	-6.7687E-02	.6988
21	.210	.6648	1.5603E-01	.2994	-7.0275E-02	.7014
22	.220	.6666	1.5584E-01	.3129	-7.3158E-02	.7030
23	.230	.6673	1.5552E-01	.3269	-7.6182E-02	.7036
24	.240	.6672	1.5470E-01	.3414	-7.9154E-02	.7030
25	.250	.6665	1.5327E-01	.3563	-8.1926E-02	.7017
26	.260	.6656	1.5126E-01	.3715	-8.4416E-02	.7000
27	.270	.6646	1.4877E-01	.3869	-8.6600E-02	.6979
28	.280	.6637	1.4592E-01	.4024	-8.8486E-02	.6958
29	.290	.6628	1.4283E-01	.4181	-9.0091E-02	.6936
30	.300	.6621	1.3956E-01	.4338	-9.1440E-02	.6915
31	.310	.6615	1.3619E-01	.4496	-9.2555E-02	.6896
32	.320	.6610	1.3276E-01	.4653	-9.3458E-02	.6877
33	.330	.6606	1.2931E-01	.4811	-9.4169E-02	.6859
34	.340	.6603	1.2585E-01	.4969	-9.4704E-02	.6843
35	.350	.6600	1.2241E-01	.5126	-9.5074E-02	.6827
36	.360	.6598	1.1899E-01	.5284	-9.5291E-02	.6813
37	.370	.6597	1.1561E-01	.5442	-9.5364E-02	.6799
38	.380	.6596	1.1226E-01	.5599	-9.5298E-02	.6787
39	.390	.6595	1.0895E-01	.5756	-9.5100E-02	.6775
40	.400	.6594	1.0568E-01	.5914	-9.4773E-02	.6764
41	.410	.6594	1.0244E-01	.6071	-9.4320E-02	.6753
42	.420	.6594	9.9248E-02	.6228	-9.3744E-02	.6743
44	.440	.6594	9.2959E-02	.6542	-9.2230E-02	.6725
45	.450	.6595	8.9865E-02	.6699	-9.1294E-02	.6717
46	.460	.6595	8.6799E-02	.6856	-9.0236E-02	.6709
47	.470	.6596	8.3767E-02	.7013	-8.9064E-02	.6702

Table II.- Continued.

(d) Concluded

	$\frac{\alpha\theta}{\Delta U}$	$\frac{c_r}{\Delta U}$	$\frac{c_i}{\Delta U}$	$\alpha_r\theta$	$\alpha_i\theta$	$\frac{c_{ph}}{\Delta U}$
48	0.480	0.6596	8.0763E-02	0.7169	-8.7776E-02	0.6695
49	.490	.6597	7.7785E-02	.7325	-8.6370E-02	.6689
50	.500	.6608	7.4986E-02	.7470	-8.4769E-02	.6693
51	.510	.6609	7.2068E-02	.7626	-8.3151E-02	.6688
52	.520	.6611	6.9174E-02	.7781	-8.1421E-02	.6683
53	.530	.6612	6.6307E-02	.7936	-7.9583E-02	.6679
54	.540	.6614	6.3463E-02	.8090	-7.7635E-02	.6675
55	.550	.6615	6.0643E-02	.8245	-7.5580E-02	.6671
56	.560	.6617	5.7847E-02	.8399	-7.3420E-02	.6668
57	.570	.6619	5.5075E-02	.8552	-7.1158E-02	.6665
58	.580	.6621	5.2326E-02	.8705	-6.8794E-02	.6663
59	.590	.6624	4.9601E-02	.8858	-6.6331E-02	.6661
60	.600	.6626	4.6898E-02	.9010	-6.3770E-02	.6659
61	.610	.6629	4.4220E-02	.9162	-6.1116E-02	.6658
62	.620	.6631	4.1563E-02	.9313	-5.8368E-02	.6658

Table II. - Continued.

(e) x/D_p = 4, axisymmetric mode (m = 0)

	$\frac{\alpha\theta}{\Delta U}$	$\frac{c_r}{\Delta U}$	$\frac{c_i}{\Delta U}$	$\alpha_r\theta$	$\alpha_i\theta$	$\frac{c_{ph}}{\Delta U}$
1	0.010	0.9924	7.0479E-03	0.0101	-7.1556E-05	0.9925
2	.020	.9851	1.9571E-02	.0203	-4.0323E-04	.9854
3	.030	.9773	3.4148E-02	.0307	-1.0712E-03	.9785
4	.040	.9686	5.0451E-02	.0412	-2.1450E-03	.9713
5	.050	.9583	6.8483E-02	.0519	-3.7099E-03	.9632
6	.060	.9450	8.8172E-02	.0629	-5.8731E-03	.9532
7	.070	.9270	-1.0818E-01	.0745	8.6935E-03	.9397
8	.080	.9024	-1.2642E-01	.0869	1.2179E-02	.9202
9	.090	.8721	-1.3759E-01	.1007	1.5885E-02	.8938
10	.100	.8393	1.3838E-01	.1160	-1.9125E-02	.8621
11	.110	.8141	1.3159E-01	.1317	-2.1286E-02	.8353
12	.120	.7951	1.2234E-01	.1474	-2.2686E-02	.8139
13	.130	.7808	1.1294E-01	.1631	-2.3588E-02	.7972
14	.140	.7699	1.0424E-01	.1786	-2.4176E-02	.7840
15	.150	.7613	9.6446E-02	.1939	-2.4566E-02	.7735
16	.160	.7544	8.9541E-02	.2091	-2.4824E-02	.7650
17	.170	.7487	8.3443E-02	.2243	-2.4996E-02	.7580
18	.180	.7439	7.8045E-02	.2393	-2.5107E-02	.7521
19	.190	.7440	7.2272E-02	.2530	-2.4573E-02	.7511
20	.200	.7406	6.7795E-02	.2678	-2.4515E-02	.7468
21	.210	.7376	6.3764E-02	.2826	-2.4430E-02	.7431
22	.220	.7350	6.0118E-02	.2973	-2.4323E-02	.7399
23	.230	.7326	5.6801E-02	.3121	-2.4196E-02	.7370
24	.240	.7305	5.3764E-02	.3268	-2.4050E-02	.7345
25	.250	.7286	5.0976E-02	.3414	-2.3889E-02	.7322
26	.260	.7269	4.8395E-02	.3561	-2.3709E-02	.7301
27	.270	.7253	4.5999E-02	.3708	-2.3513E-02	.7282
28	.280	.7223	4.4796E-02	.3862	-2.3948E-02	.7251
29	.290	.7225	4.1660E-02	.4000	-2.3066E-02	.7249
30	.300	.7213	3.9682E-02	.4147	-2.2813E-02	.7235
31	.310	.7201	3.7807E-02	.4293	-2.2539E-02	.7221
32	.320	.7190	3.6024E-02	.4439	-2.2243E-02	.7208
33	.330	.7180	3.4319E-02	.4586	-2.1921E-02	.7196
34	.340	.7170	3.2688E-02	.4732	-2.1576E-02	.7185
35	.350	.7160	3.1119E-02	.4879	-2.1205E-02	.7174
36	.360	.7151	2.9601E-02	.5026	-2.0804E-02	.7163
37	.370	.7142	2.8135E-02	.5173	-2.0378E-02	.7153
38	.380	.7133	2.6710E-02	.5320	-1.9921E-02	.7143
39	.390	.7124	2.5324E-02	.5467	-1.9434E-02	.7133
40	.400	.7116	2.3974E-02	.5615	-1.8918E-02	.7124
41	.410	.7107	2.2656E-02	.5763	-1.8371E-02	.7114
42	.420	.7099	2.1371E-02	.5911	-1.7797E-02	.7105
43	.430	.7090	2.0112E-02	.6060	-1.7190E-02	.7096
44	.440	.7081	1.8885E-02	.6209	-1.6558E-02	.7086
45	.450	.7073	1.7683E-02	.6359	-1.5898E-02	.7077
46	.460	.7064	1.6512E-02	.6509	-1.5214E-02	.7068
47	.470	.7055	1.5369E-02	.6659	-1.4507E-02	.7058

Table II. - Continued.

(f) x/D_p = 4, First azimuthal mode (m = 1)

	$\frac{\alpha\theta}{\Delta U}$	$\frac{c_r}{\Delta U}$	$\frac{c_i}{\Delta U}$	$\alpha_r\theta$	$\alpha_i\theta$	$\frac{c_{ph}}{\Delta U}$
1	0.010	0.5397	2.3323E-01	0.0156	-6.7473E-03	0.6405
2	.020	.5398	2.2889E-01	.0314	-1.3318E-02	.6368
3	.030	.5404	2.2196E-01	.0475	-1.9509E-02	.6316
4	.040	.5423	2.1306E-01	.0639	-2.5106E-02	.6260
5	.050	.5457	2.0310E-01	.0805	-2.9955E-02	.6213
6	.060	.5505	1.9298E-01	.0971	-3.4027E-02	.6181
7	.070	.5563	1.8332E-01	.1135	-3.7399E-02	.6167
8	.080	.5627	1.7437E-01	.1297	-4.0193E-02	.6168
9	.090	.5693	1.6619E-01	.1457	-4.2526E-02	.6178
10	.100	.5758	1.5871E-01	.1614	-4.4489E-02	.6196
11	.110	.5821	1.5184E-01	.1769	-4.6150E-02	.6217
12	.120	.5881	1.4548E-01	.1923	-4.7560E-02	.6241
13	.130	.5938	1.3954E-01	.2075	-4.8754E-02	.6266
14	.140	.5991	1.3395E-01	.2225	-4.9755E-02	.6291
15	.150	.6041	1.2866E-01	.2375	-5.0581E-02	.6315
16	.160	.6088	1.2361E-01	.2524	-5.1246E-02	.6339
17	.170	.6132	1.1876E-01	.2672	-5.1757E-02	.6362
18	.180	.6172	1.1407E-01	.2820	-5.2121E-02	.6383
19	.190	.6210	1.0953E-01	.2967	-5.2340E-02	.6403
20	.200	.6245	1.0510E-01	.3114	-5.2418E-02	.6422
21	.210	.6277	1.0077E-01	.3261	-5.2355E-02	.6439
22	.220	.6308	9.6526E-02	.3408	-5.2153E-02	.6455
23	.230	.6336	9.2342E-02	.3555	-5.1807E-02	.6470
24	.240	.6362	8.8216E-02	.3701	-5.1319E-02	.6484
25	.250	.6387	8.4135E-02	.3848	-5.0687E-02	.6498
26	.260	.6410	8.0092E-02	.3994	-4.9908E-02	.6510
27	.270	.6431	7.6083E-02	.4140	-4.8984E-02	.6521
28	.280	.6451	7.2100E-02	.4287	-4.7910E-02	.6532
29	.290	.6470	6.8139E-02	.4433	-4.6686E-02	.6542
30	.300	.6488	6.4197E-02	.4579	-4.5311E-02	.6551
31	.310	.6505	6.0273E-02	.4725	-4.3784E-02	.6561
32	.320	.6521	5.6365E-02	.4871	-4.2106E-02	.6569
33	.330	.6536	5.2471E-02	.5017	-4.0276E-02	.6578
34	.340	.6550	4.8588E-02	.5162	-3.8293E-02	.6586
35	.350	.6564	4.4718E-02	.5308	-3.6159E-02	.6594
36	.360	.6577	4.0860E-02	.5453	-3.3873E-02	.6602
37	.370	.6590	3.7008E-02	.5597	-3.1434E-02	.6610
38	.380	.6602	3.3168E-02	.5742	-2.8846E-02	.6618
39	.390	.6613	2.9331E-02	.5886	-2.6104E-02	.6626
40	.400	.6624	2.5498E-02	.6030	-2.3209E-02	.6634
41	.410	.6635	2.1669E-02	.6173	-2.0162E-02	.6642
42	.420	.6644	1.7847E-02	.6317	-1.6967E-02	.6649

Table II. - Continued.

(g) x/D_p = 8, First azimuthal mode (m = 1)

	$\frac{\alpha\theta}{\Delta U}$	$\frac{c_r}{\Delta U}$	$\frac{c_i}{\Delta U}$	$\alpha_r\theta$	$\alpha_i\theta$	$\frac{c_{ph}}{\Delta U}$
1	0.010	0.5134	1.0511E-01	0.0187	-3.8279E-03	0.5349
2	.020	.5136	1.0493E-01	.0374	-7.6372E-03	.5350
3	.030	.5140	1.0464E-01	.0560	-1.1410E-02	.5353
4	.040	.5145	1.0424E-01	.0747	-1.5129E-02	.5356
5	.050	.5151	1.0389E-01	.0933	-1.8811E-02	.5361
6	.060	.5159	1.0328E-01	.1118	-2.2384E-02	.5366
7	.070	.5169	1.0259E-01	.1303	-2.5862E-02	.5372
8	.080	.5179	1.0183E-01	.1487	-2.9236E-02	.5380
9	.090	.5191	1.0099E-01	.1670	-3.2497E-02	.5388
10	.100	.5204	1.0010E-01	.1853	-3.5640E-02	.5397
11	.110	.5218	9.9152E-02	.2035	-3.8662E-02	.5406
12	.120	.5233	9.8164E-02	.2215	-4.1560E-02	.5417
13	.130	.5248	9.7142E-02	.2395	-4.4334E-02	.5428
14	.140	.5264	9.6092E-02	.2574	-4.6985E-02	.5439
15	.150	.5265	9.7005E-02	.2755	-5.0764E-02	.5444
16	.160	.5282	9.5880E-02	.2932	-5.3228E-02	.5456
17	.170	.5300	9.4739E-02	.3108	-5.5570E-02	.5469
18	.180	.5317	9.3591E-02	.3284	-5.7795E-02	.5482
19	.190	.5335	9.2434E-02	.3458	-5.9903E-02	.5495
20	.200	.5353	9.1269E-02	.3631	-6.1899E-02	.5509
21	.210	.5371	9.0103E-02	.3803	-6.3786E-02	.5523
22	.220	.5390	8.8932E-02	.3974	-6.5567E-02	.5536
23	.230	.5408	8.7763E-02	.4144	-6.7246E-02	.5550
24	.240	.5426	8.6591E-02	.4313	-6.8825E-02	.5565
25	.250	.5445	8.5420E-02	.4481	-7.0306E-02	.5579
26	.260	.5463	8.4248E-02	.4649	-7.1693E-02	.5593
27	.270	.5481	8.3077E-02	.4815	-7.2988E-02	.5607
28	.280	.5499	8.1905E-02	.4981	-7.4192E-02	.5621
29	.290	.5517	8.0733E-02	.5146	-7.5309E-02	.5635
30	.300	.5535	7.9561E-02	.5311	-7.6338E-02	.5649
31	.310	.5552	7.8391E-02	.5474	-7.7285E-02	.5663
32	.320	.5570	7.7219E-02	.5637	-7.8147E-02	.5677
33	.330	.5587	7.6046E-02	.5799	-7.8929E-02	.5691
34	.340	.5604	7.4874E-02	.5960	-7.9630E-02	.5704
35	.350	.5621	7.3700E-02	.6121	-8.0254E-02	.5718
36	.360	.5638	7.2527E-02	.6281	-8.0800E-02	.5731
37	.370	.5655	7.1350E-02	.6441	-8.1268E-02	.5745
38	.380	.5671	7.0174E-02	.6600	-8.1662E-02	.5758
39	.390	.5687	6.8994E-02	.6758	-8.1980E-02	.5771
40	.400	.5703	6.7815E-02	.6916	-8.2227E-02	.5784
41	.420	.5735	6.5447E-02	.7229	-8.2497E-02	.5810
42	.440	.5766	6.3073E-02	.7541	-8.2484E-02	.5835
43	.460	.5796	6.0689E-02	.7850	-8.2190E-02	.5860
44	.480	.5826	5.8297E-02	.8157	-8.1622E-02	.5884
45	.500	.5855	5.5897E-02	.8462	-8.0785E-02	.5909
46	.520	.5884	5.3489E-02	.8765	-7.9686E-02	.5932
47	.540	.5912	5.1071E-02	.9067	-7.8324E-02	.5956
48	.560	.5939	4.8644E-02	.9366	-7.6707E-02	.5979

Table II. - Continued.

(g) Concluded

	$\frac{\alpha\theta}{\Delta U}$	$\frac{c_r}{\Delta U}$	$\frac{c_i}{\Delta U}$	$\alpha_r\theta$	$\alpha_i\theta$	$\frac{c_{ph}}{\Delta U}$
49	0.580	0.5966	4.6209E-02	0.9663	-7.4839E-02	0.6002
50	.600	.5993	4.3762E-02	.9958	-7.2715E-02	.6025
51	.620	.6020	4.1314E-02	1.0251	-7.0358E-02	.6048
52	.640	.6046	3.8893E-02	1.0542	-6.7819E-02	.6071
53	.660	.6071	3.6530E-02	1.0832	-6.5170E-02	.6093
54	.680	.6107	3.3531E-02	1.1101	-6.0950E-02	.6126
55	.700	.6138	3.0811E-02	1.1375	-5.7094E-02	.6154
56	.720	.6163	2.8389E-02	1.1658	-5.3700E-02	.6176
57	.740	.6187	2.5967E-02	1.1939	-5.0105E-02	.6198
58	.760	.6211	2.3545E-02	1.2218	-4.6313E-02	.6220
59	.780	.6235	2.1122E-02	1.2495	-4.2327E-02	.6242

Table II. - Concluded.

(h) x/D_p = 12.75, First azimuthal mode (m = 1)

	$\frac{\alpha\theta}{\Delta U}$	$\frac{c_r}{\Delta U}$	$\frac{c_i}{\Delta U}$	$\alpha_r\theta$	$\alpha_i\theta$	$\frac{c_{ph}}{\Delta U}$
1	0.010	0.4674	9.1103E-02	0.0206	-4.0172E-03	0.4852
2	.020	.4687	8.9350E-02	.0412	-7.8478E-03	.4858
3	.030	.4710	8.6597E-02	.0616	-1.1329E-02	.4869
4	.040	.4741	8.3063E-02	.0819	-1.4343E-02	.4886
5	.050	.4780	7.9004E-02	.1018	-1.6828E-02	.4911
6	.060	.4827	7.4662E-02	.1214	-1.8778E-02	.4942
7	.070	.4879	7.0230E-02	.1406	-2.0231E-02	.4980
8	.080	.4936	6.5835E-02	.1592	-2.1241E-02	.5024
9	.090	.4995	6.1550E-02	.1775	-2.1871E-02	.5071
10	.100	.5056	5.7407E-02	.1953	-2.2175E-02	.5121
11	.110	.5117	5.3408E-02	.2127	-2.2199E-02	.5172
12	.120	.5178	4.9547E-02	.2297	-2.1978E-02	.5225
13	.130	.5238	4.5810E-02	.2463	-2.1542E-02	.5278
14	.140	.5297	4.2177E-02	.2626	-2.0911E-02	.5331
15	.150	.5355	3.8632E-02	.2786	-2.0100E-02	.5383
16	.160	.5412	3.5162E-02	.2944	-1.9124E-02	.5435
17	.170	.5468	3.1751E-02	.3098	-1.7991E-02	.5487
18	.180	.5523	2.8390E-02	.3251	-1.6711E-02	.5537
19	.190	.5576	2.5074E-02	.3401	-1.5292E-02	.5587
20	.200	.5628	2.1791E-02	.3548	-1.3739E-02	.5636
21	.210	.5679	1.8537E-02	.3694	-1.2058E-02	.5685
22	.220	.5729	1.5312E-02	.3838	-1.0257E-02	.5733
23	.230	.5777	1.2106E-02	.3979	-8.3379E-03	.5780
24	.240	.5825	8.9219E-03	.4119	-6.3087E-03	.5827
25	.250	.5825	5.4729E-03	.4291	-4.0318E-03	.5826
26	.260	.5826	5.4729E-03	.4463	-4.1922E-03	.5826
27	.270	.5823	4.8219E-03	.4637	-3.8396E-03	.5823

TABLE III. - PRIMARY STREAM EIGENVALUES, GROWTH RATES, AND PHASE VELOCITIES

x/θ_p = 1, First order azimuthal mode (m = 1)

	$\frac{\alpha\theta}{\Delta U}$	$\frac{c_r}{\Delta U}$	$\frac{c_i}{\Delta U}$	$\alpha_r\theta$	$\alpha_i\theta$	$\frac{c_{ph}}{\Delta U}$
1	0.010	0.4959	4.0110E-01	0.0122	-9.8603E-03	0.8203
2	.020	.5179	3.7239E-01	.0255	-1.8306E-02	.7856
3	.030	.5409	3.6217E-01	.0383	-2.5643E-02	.7834
4	.040	.5502	3.6127E-01	.0508	-3.3353E-02	.7874
5	.050	.5472	3.6163E-01	.0636	-4.2025E-02	.7862
6	.060	.5349	3.5945E-01	.0773	-5.1931E-02	.7764
7	.070	.5157	3.5235E-01	.0925	-6.3233E-02	.7564
8	.080	.4921	3.3797E-01	.1105	-7.5874E-02	.7242
9	.090	.4684	3.1396E-01	.1326	-8.8877E-02	.6788
10	.100	.4511	2.8162E-01	.1595	-9.9578E-02	.6269
11	.110	.4434	2.4722E-01	.1893	-1.0554E-01	.5812
12	.120	.4427	2.1553E-01	.2191	-1.0670E-01	.5476
13	.130	.4459	1.8773E-01	.2477	-1.0427E-01	.5249
14	.140	.4540	1.6553E-01	.2722	-9.9225E-02	.5144
15	.145	.4569	1.5452E-01	.2848	-9.6302E-02	.5092
16	.150	.4602	1.4583E-01	.2962	-9.3866E-02	.5064
17	.160	.4647	1.2396E-01	.3214	-8.5747E-02	.4978

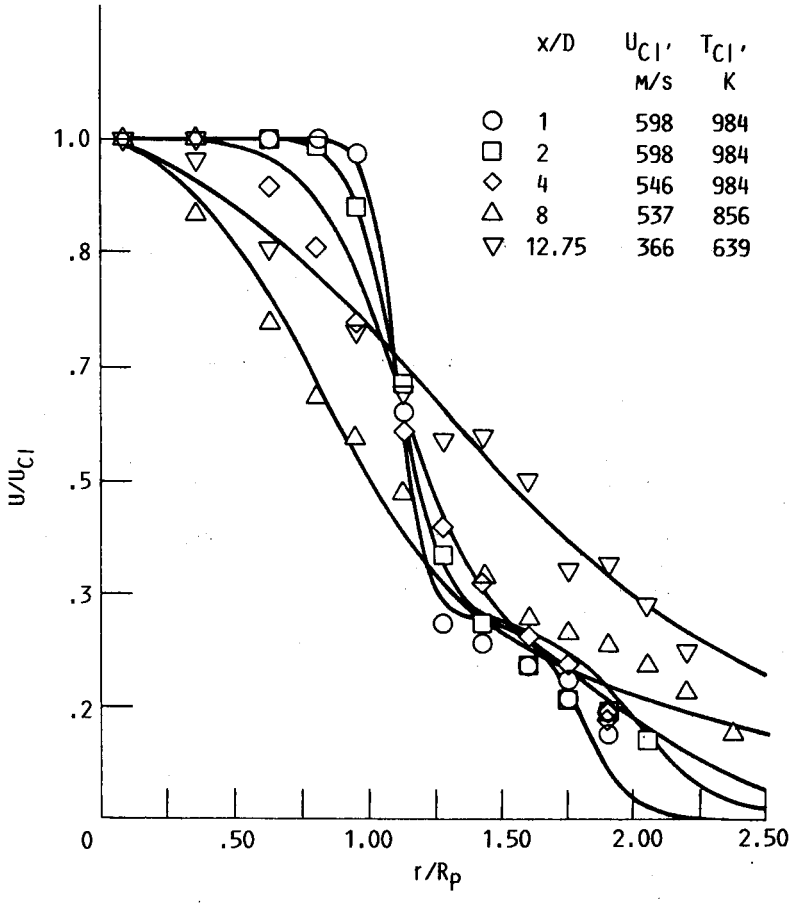

FIGURE 1.- COMPARISON OF CALCULATED AND MEASURED RADIAL VELOCITY PROFILES FOR: U_S/U_P RATIO OF 0.3; NOZZLE AREA RATIO, 1.9; T_P, 984 K; T_S, 285 K; U_P, 598 m/s; U_S, 174 m/s.

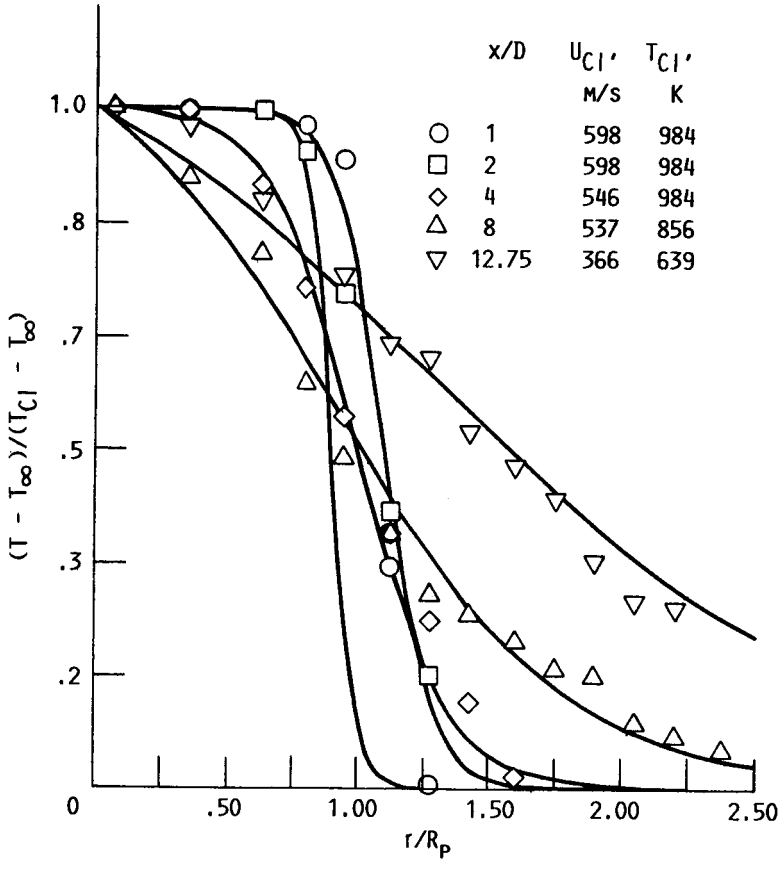

FIGURE 2.- COMPARISON OF CALCULATED AND MEASURED RADIAL TEMPERATURE PROFILES FOR: U_S/U_P RATIO OF 0.3; NOZZLE AREA RATIO, 1.9; T_P, 984 K; T_S, 285 K; U_P, 598 m/s; U_S, 174 m/s.

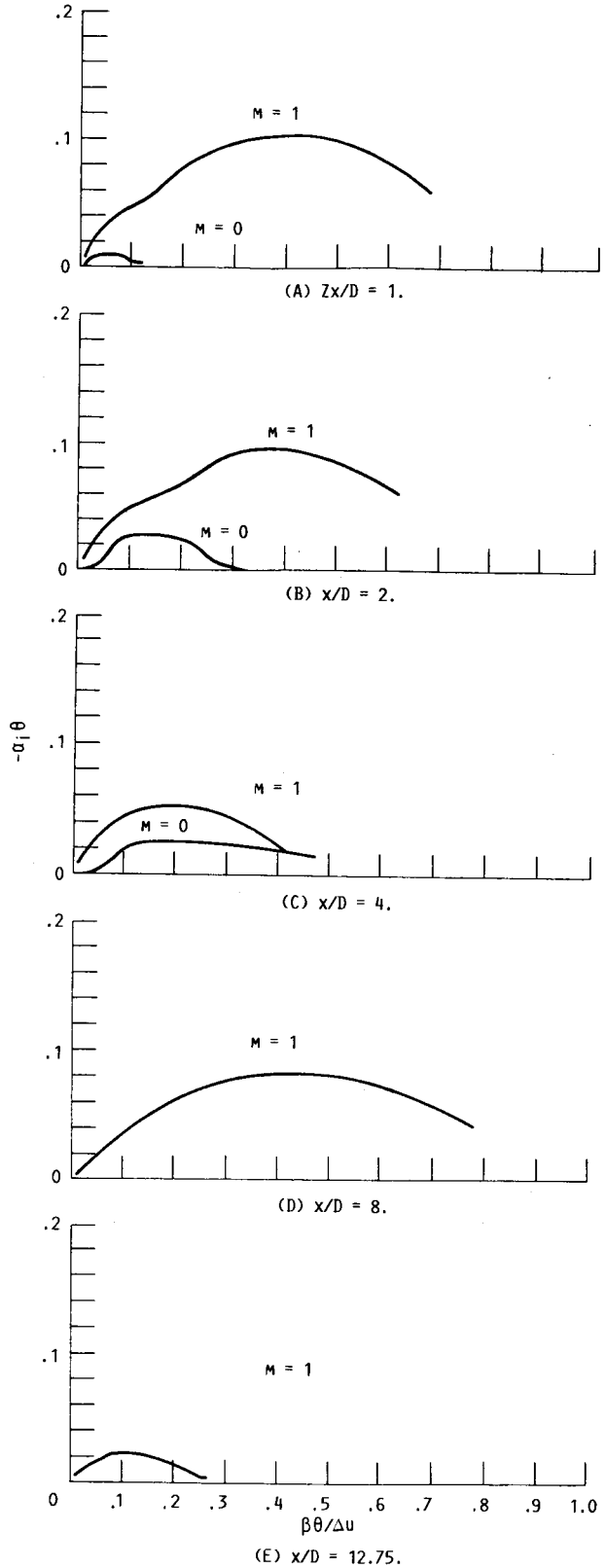

FIGURE 3.- SPATIAL GROWTH RATE OF THE AXISYMMETRIC (M = 0) AND FIRST AZIMUTHAL (M = 1) DISTURBANCE.

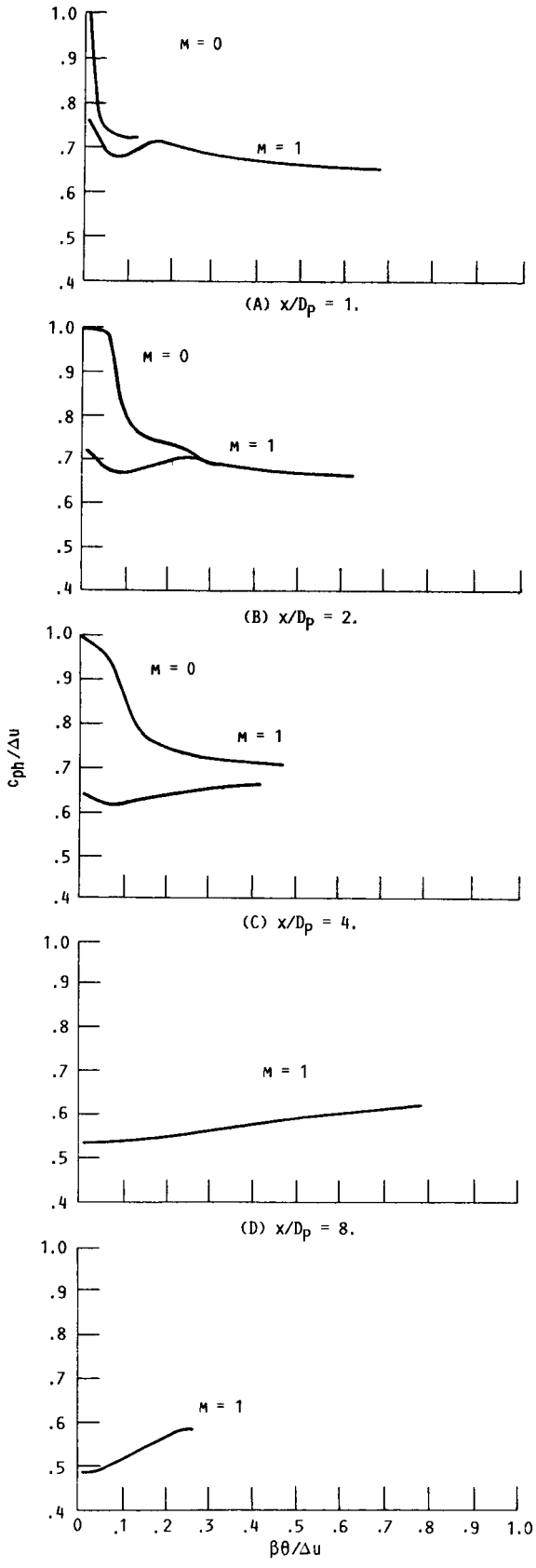

FIGURE 4.- AXIAL PHASE VELOCITY OF THE AXISYMMETRIC (M = 0) AND FIRST AXIMUTHAL (M = 1) DISTURBANCE.

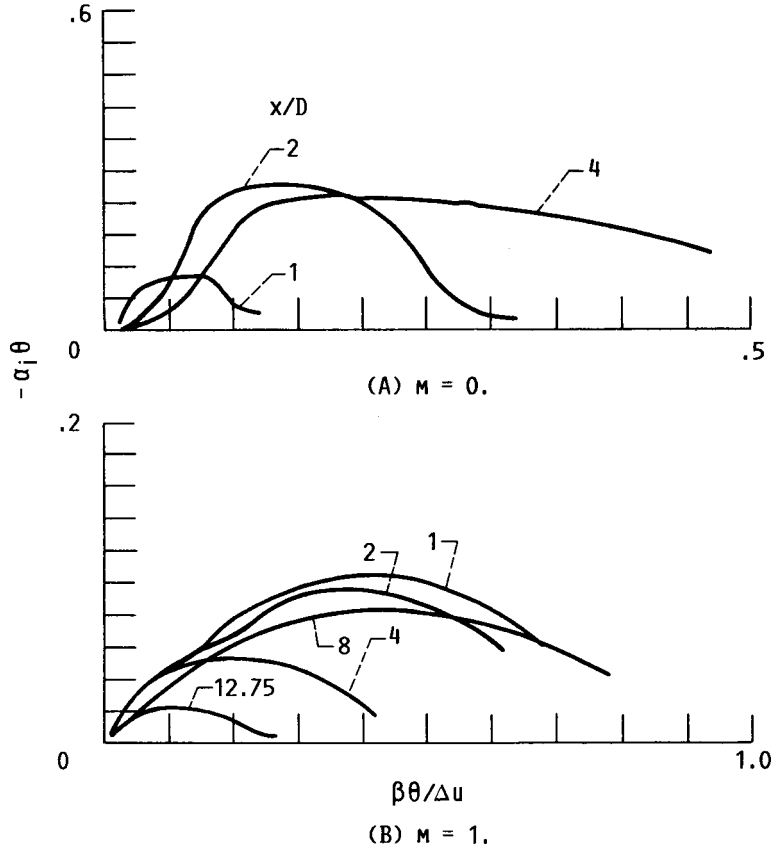

FIGURE 5.- SPATIAL GROWTH RATE AT VARIOUS x/D_p.

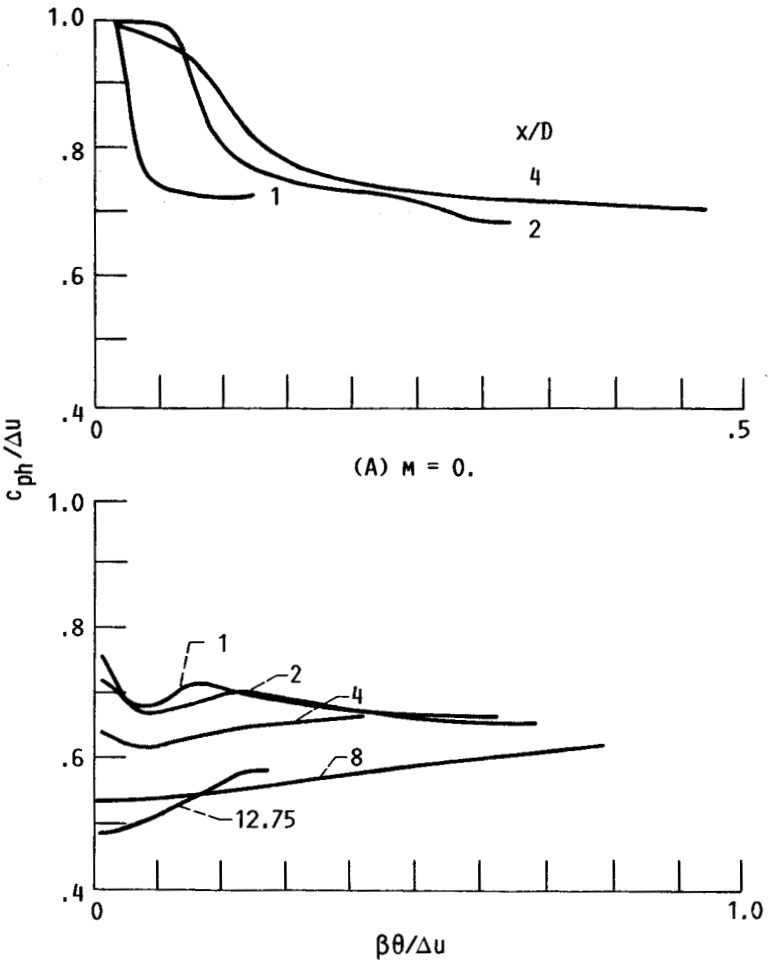

FIGURE 6.- PHASE VELOCITY AT VARIOUS x/D.

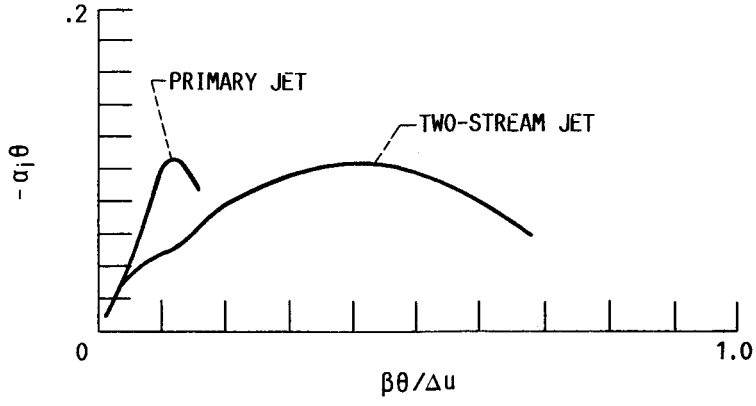

FIGURE 7.- COMPARISON OF SPATIAL GROWTH RATE OF THE FIRST AZIMUTHAL (M = 1) DISTURBANCE AT x/D = 1 FOR PRIMARY JET WITH AND WITHOUT SECONDARY FLOW.

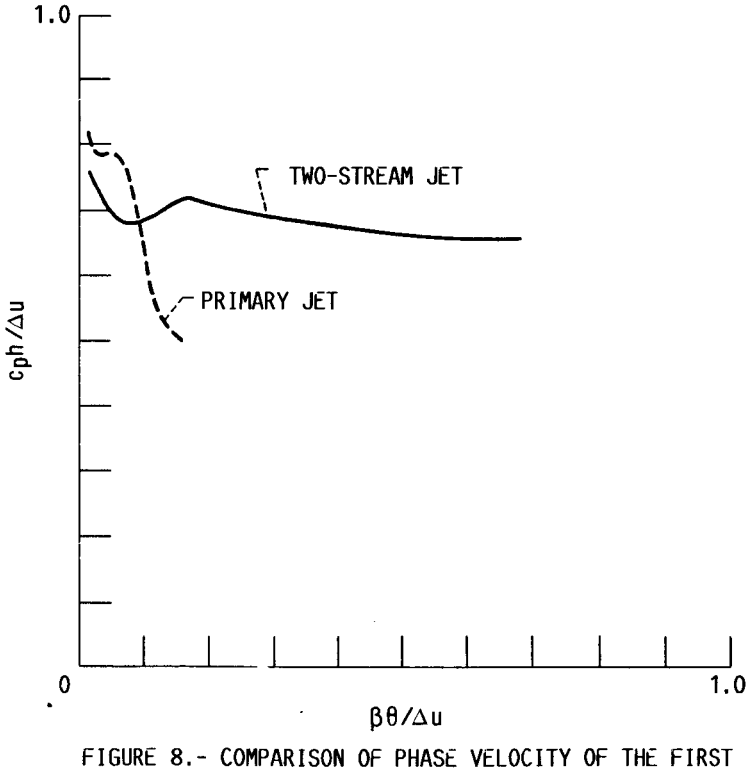

FIGURE 8.- COMPARISON OF PHASE VELOCITY OF THE FIRST AZIMUTHAL (M = 1) DISTURBANCE AT x/D = 1 FOR PRIMARY JET WITH AND WITHOUT SECONDARY FLOW.